

Plasma Generation Near an Ion Thruster Discharge Chamber Hollow Cathode

Ira Katz[†], John R. Anderson*, Dan M. Goebel**, Richard Wirz[‡], Anita Sengupta*
*Jet Propulsion Laboratory
California Institute of Technology
Pasadena, California*

In gridded electrostatic thrusters, ions are produced by electron bombardment in the discharge chamber. In most of these thrusters, a single, centrally located hollow cathode supplies the ionizing electrons. An applied magnetic field in the discharge chamber restricts the electrons leaving the hollow cathode to a very narrow channel. In this channel, the high electron current density ionizes both propellant gas flowing from the hollow cathode, and other neutrals from the main propellant flow from the plenum. The processes that occur just past the hollow cathode exit are very important. In recent engine tests, several cases of discharge cathode orifice plate and keeper erosion have been reported. In this paper we present results from a new 1-D, variable area model of the plasma processes in the magnetized channel just downstream of the hollow cathode keeper. The model predicts plasma densities and temperatures consistent with those reported in the literature for the NSTAR engine, and preliminary results from the model show a potential maximum just downstream of the cathode.

Introduction

Thruster life is one of the most important parameters in applying electric propulsion devices on spacecraft. Most of the previous work has focused on grid erosion as the major life limiting phenomenon. However, in recent years the understanding of grid erosion and the predictive capabilities of multidimensional simulation codes has led to grid designs and materials adequate to meet most mission life requirements. During the wear tests of the NSTAR ion thruster¹⁻⁵, discharge chamber cathode and cathode keeper erosion has arisen as an important life concern for thruster life. There have been several experimental

investigations into the plasma processes near the discharge cathode and measurements of wear rates⁶⁻¹⁰. In the process of developing a full 2-D model of the discharge chamber plasma, we have investigated the plasma parameters locally near the cathode exit using a simple, one-dimensional fluid model. In this paper, we present the plasma parameters near the discharge cathode predicted by the model.

This new model includes electrons as well as neutral, singly ionized, and doubly ionized xenon atoms. The electron energy equation is solved to balance Ohmic heating with ion production, radiation, convection, and conduction. First results show that there is region of high electron drift velocity just a few millimeters downstream of the keeper. In this region, the plasma electrons undergo rapid

[†]Supervisor, Advanced Propulsion Technology Group, Member AIAA,

*Member Technical Staff, Member AIAA

**Section Staff, Member AIAA

[‡]Graduate Student, California Institute of Technology

heating, and there is significant ionization of the gas flowing from the cathode and discharge chamber by the electron stream. However, the fraction of doubly-ionized xenon atoms produced in this region is very low due to the high single ion production rate and the short ion residence time. The model predicts a strong electric field is present that accelerates ions from this plasma back toward the cathode and keeper. A potential peak, as posited previously¹¹⁻¹³, is also observed, with significant double ion production occurring downstream of the peak where the gas density is low. The details of this region are shown to control discharge chamber hollow cathode orifice plate and keeper erosion.

Background

During the first wear test of the NSTAR 30 cm ion thruster¹, two discharge chamber hollow cathode assemblies were used—one for the first 867 hours and the second for the last 1164 hours of the test, which was voluntarily terminated at 2031 hours. Examination of both cathode assemblies, after testing, revealed substantial erosion of the outer edge of discharge cathode orifice plate, heater wire and thermal radiation shielding. Several design changes were made to fix the erosion problem²; changes included moving the heater wire so that it did not extend downstream of the orifice plate and the cathode assemble was enclosed within a cylindrical keeper electrode. After a 1000 hour test was conducted on the new design at ~25% higher cathode flow rate (due to a calibration error), no erosion was observed at the outer edge of the orifice plate but the keeper thickness changed by 25-75 μm^2 . During the subsequent 8000 hour test³, erosion was observed on the inner diameter and the downstream surface of the keeper; the maximum eroded depth on the keeper face was ~530 μm or about 1/3 of the keeper thickness. Both the design changes and the

higher flow rate were used on the NSTAR thruster that flew successfully on Deep Space One⁴.

However, during the subsequent Extended Life Test of the NSTAR flight spare thruster, the severe erosion of the keeper electrode was observed⁵. During the first 4693 hours of the test, which was conducted mostly at the full power point, photographs show surface texturing consistent with the keeper erosion observed during the 8000 hour test. Between 4693 and 10451 hours, the thruster was operated at the NSTAR half power point and the keeper orifice eroded to the point where the entire cathode orifice plate and about half of the heater wire were exposed to the discharge chamber plasma. Full power operation was resumed between 10451 and 15617 hours and the keeper orifice continued to erode; at the end of this full power segment, the entire heater wire and radiation shielding were exposed to the discharge chamber plasma. Testing at the NSTAR minimum power point was conducted between 15617 and 21306 hours, and the keeper orifice continued to erode, albeit at a lower rate. Testing of the thruster continued until 30,352 hours when test was voluntarily terminated. Post test inspection showed that the orifice plate erosion was more significant at larger radii, the heater wire was significantly eroded and the keeper electrode face had been completely eroded away.

Several groups have performed investigations to try to understand the mechanisms that caused the erosion of the NSTAR discharge cathode keeper. Williams used laser-induced fluorescence (LIF) to measure relative erosion rates and plasma ion velocity vectors in the vicinity of the discharge cathode in a 30 cm ion engine⁶. He concluded that a potential hill downstream of the cathode accelerated ions back to the cathode and caused the erosion. Foster measured radial plasma density and

potential profiles near the keeper⁷. Domonkos measure erosion of a copper keeper⁸. Kolisinki used surface layer activation of molybdenum keepers to obtain keeper erosion rates for a range of operating parameters⁹. Herman measured plasma densities and temperatures in the 30 cm discharge chamber¹⁰. Predictions of the plasma density from the 1-D model presented here compare well with the measured center line axial densities in these references when the same operating conditions are analyzed.

Model

Figure 1 shows a visible wavelength photograph of the discharge chamber of the NSTAR flight spare thruster operating in the JPL Extended Life Test. The figure shows the bright plasma region characteristically observed near the cathode exit, in addition to the neutralizer cathode in the upper right corner. Figure 2 shows the same photograph, but digitally enhanced to resolve the intense source of light directly in front of the discharge cathode. It is the first few centimeters of this region that the present 1-D model is designed to simulate. The model assumes that the discharge current is carried by a drifted Maxwellian distribution of electrons from the cathode orifice region. The electrons are confined by an axial magnetic field to a narrow column. The axial magnetic field in this region varies in from about 100 Gauss at the orifice exit to tens of Gauss several centimeters into the discharge chamber. The thermal electron Larmor radius in this region is much less than the column radius. The column radius is assumed to expand as the magnetic field strengths decreases, conserving magnetic flux. This assumption is only good as long as the field lines are nearly axial.

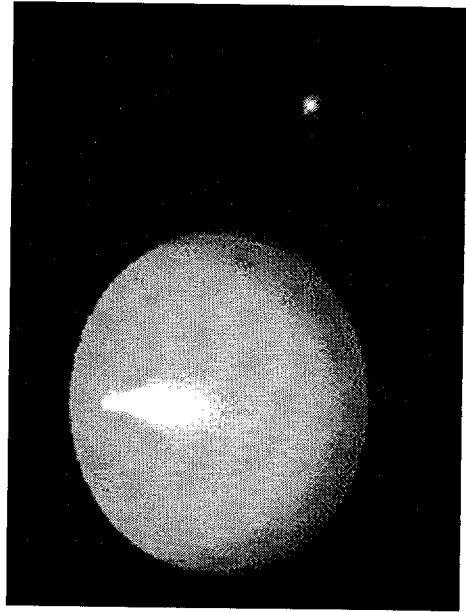


Figure 1. The discharge chamber of the NSTAR thruster. The discharge chamber cathode is the source of the large plume. The neutralizer hollow cathode is the bright dot in the upper right hand corner.

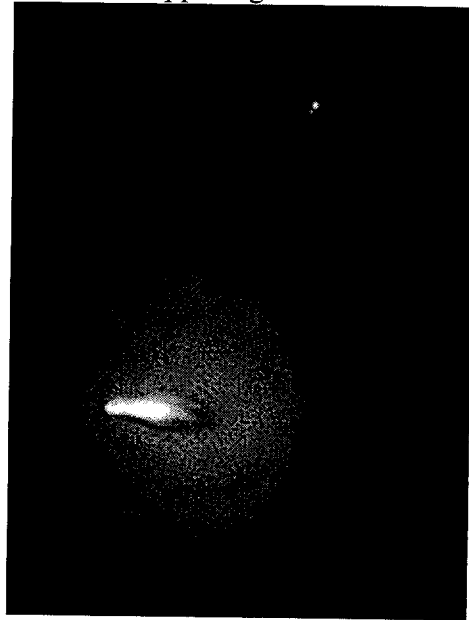


Figure 2. The discharge chamber of the NSTAR thruster enhanced to show the narrow current channel downstream of the discharge chamber hollow cathode.

The neutral gas density in the column comes from two sources. The first is a narrow jet of xenon atoms emerging from the hollow cathode. The second source is gas flowing radially inward from the discharge chamber. The magnitude of this gas is much smaller in this region than the gas from the hollow cathode. The neutral gas continuity equation is

$$n_{HC}(x) = \frac{F_{HC}}{v_{HC} \pi R_{keeper}^2} \frac{x_{HC}^2}{(x + x_{HC})^2} \exp\left(-\int_0^x \frac{n_e(x) \alpha^+(T_e(x))}{v_{HC}} dx\right)$$

$$n_0 = n_{chamber} \exp\left(-\frac{2\pi R(x) n_e \alpha^+(T_e)}{\bar{c}}\right) + n_{HC}$$

where n_{HC} is the number density due to gas coming out of the hollow cathode, F_{HC} is the mass flow rate of hollow cathode gas, v_{HC} is the bulk speed of the hollow cathode gas, πR_{keeper}^2 is the cathode keeper orifice cross-sectional area which the hollow cathode gas flows through to reach the discharge chamber, x_{HC} is the distance between the cathode orifice and the cathode keeper orifice, x is the axial distance downstream of the cathode keeper orifice, $\alpha^+(T_e(x))$ is the ionization rate per unit volume for neutrals, n_0 is the neutral gas density at a given axial location, $n_{chamber}$ is the assumed background chamber density, $R(x)$ is the radius of the column, n_e is the electron number density, and \bar{c} is the average thermal speed of the discharge chamber neutrals.

The ion continuity equations assume ambipolar diffusion axially, and radial ion loss at the ion thermal velocity. The axial diffusion rate coefficient is calculated assuming resonant charge exchange between neutrals and ions is the dominant scattering term. The mean free path for these charge exchange

events is few millimeters at the exit of the orifice and several centimeters downstream of the keeper in the discharge chamber. The ion velocity used to calculate the scattering frequency is the ion Bohm velocity

$$\nabla \cdot (n^+ \mathbf{v}) = \dot{n}^+ - \dot{n}^{++}$$

$$v_x = -D_a \frac{\partial n^+}{\partial x} \approx -\frac{\sqrt{eT_e}}{n_0 \sigma_{CEX}} \frac{\partial n^+}{\partial x}$$

$$v_r = \sqrt{\frac{eT_i}{m_i}}$$

$$\dot{n}^+ = n_0 n_e \alpha^+(T_e)$$

$$\dot{n}^{++} = n^+ n_e \alpha^{++}(T_e)$$

where n^+ is the single ion number density, \dot{n}^+ is the single ion production rate, \dot{n}^{++} is the double ion production rate (for production of double ions from single ions), v_x is the axial speed of ions at a given location, D_a is the ambipolar diffusion coefficient, e is the electron charge, T_e is the electron temperature, m_i is the ion mass, T_i is the ion temperature, $\alpha^{++}(T_e)$ is the double ion production rate.

The treatment of double ions is similar to that for single ions. Double ions are produced primarily by the second ionization of Xe^+ . The charge exchange cross section for Xe^{++} is about half of that for singly charged xenon¹⁴.

$$\nabla \cdot (n^{++} \mathbf{v}) = \dot{n}^{++}$$

$$v_x = -D_a \frac{\partial n^{++}}{\partial x} \approx -\frac{\sqrt{2eT_e}}{n_0 \sigma_{CEX}} \frac{\partial n^{++}}{\partial x}$$

$$v_r = \sqrt{\frac{eT_i}{m_i}}$$

$$\dot{n}^{++} = n^+ n_e \alpha^{++}(T_e)$$

where n^{++} is the double ion number density.

The electron energy equation balances the steady state Joule heating with radiative, ionization, conductive, and convective losses:

$$0 = -\nabla \cdot \left(-\frac{5}{2} j_e T_e - \kappa \nabla T_e \right) + \eta j_e^2 - \dot{n}^+ I_p^+ - \dot{n}^{++} e I_p^{++}$$

where j_e is the electron current through the column, κ is the thermal conductivity coefficient, η is the plasma resistivity, I_p^+ is the single ionization potential, I_p^{++} is the double ionization potential. The resistivity formulation is purely classical and includes both electron neutral and electron ion scattering¹⁵.

Results

We applied the model first to the operating point TH4 of the NSTAR thruster. At this throttle point, the discharge current was set to 6.05 A and the gas flow through the cathode was set to 2.47 sccm. This operating point was chosen so the results could be compared directly to the measurements of Herman, et al¹⁰.

The choice of boundary conditions is critically important. Ideally this model would connect self-consistently with a hollow cathode model on the upstream end, and a discharge chamber model on the down stream end. In the absence of these models, we chose to set the plasma temperature upstream to 3 eV, a value consistent with our 1-D hollow cathode results¹⁵. Thermal conduction is set to zero at both ends of the computational domain. Electrons convect heat in at the upstream boundary, and convect heat out the

downstream end of the computational domain. The plasma density at the upstream end is assumed to have zero axial gradient, and at the downstream boundary the plasma density is set to the value calculated to provide the extracted ion current density at at the screen grid for the given throttle set point. The computational domain is normally 6 centimeters long.

Axial density profiles are shown in Figure 3 for operation at TH4. The single ion density ranges from $2 \times 10^{18} \text{ m}^{-3}$ down to $2 \times 10^{17} \text{ m}^{-3}$. These values are in reasonable agreement with those reported by Herman, et al¹⁰. The double ion density predictions are about 3 orders of magnitude lower than that for single ions; this is discussed further in a later section.

Axial density profiles are shown in Figure 4 for operation at TH15. The single ion density ranges from $5 \times 10^{18} \text{ m}^{-3}$ down to $2 \times 10^{17} \text{ m}^{-3}$, again in good agreement with the literature. Calculated axial potential profiles are shown in Figures 5 and 6 for operation at TH4 and TH15. A potential hill is predicted by the model just downstream of the keeper. This potential hill accelerates ions both toward the cathode/keeper structure and toward the screen grid. Energetic ions accelerated from this potential maximum are likely the source of the cathode orifice plate and keeper erosion observed in the NSTAR life tests. The magnitude and location of this potential peak depends on the operating conditions. The actual value of the plasma potential at the peak is determined by the potential drops upstream and downstream of the domain of this model. Future work will couple these results to the hollow cathode model and the discharge chamber model to determine the plasma potential in this region.

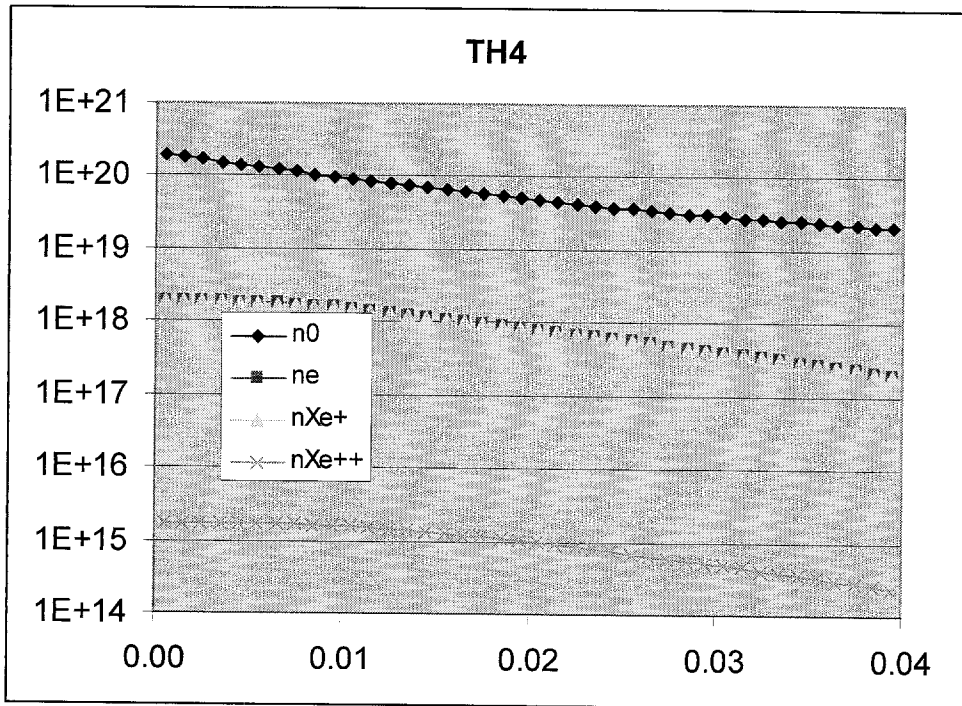


Figure 3 Model plasma densities for operating condition TH4.

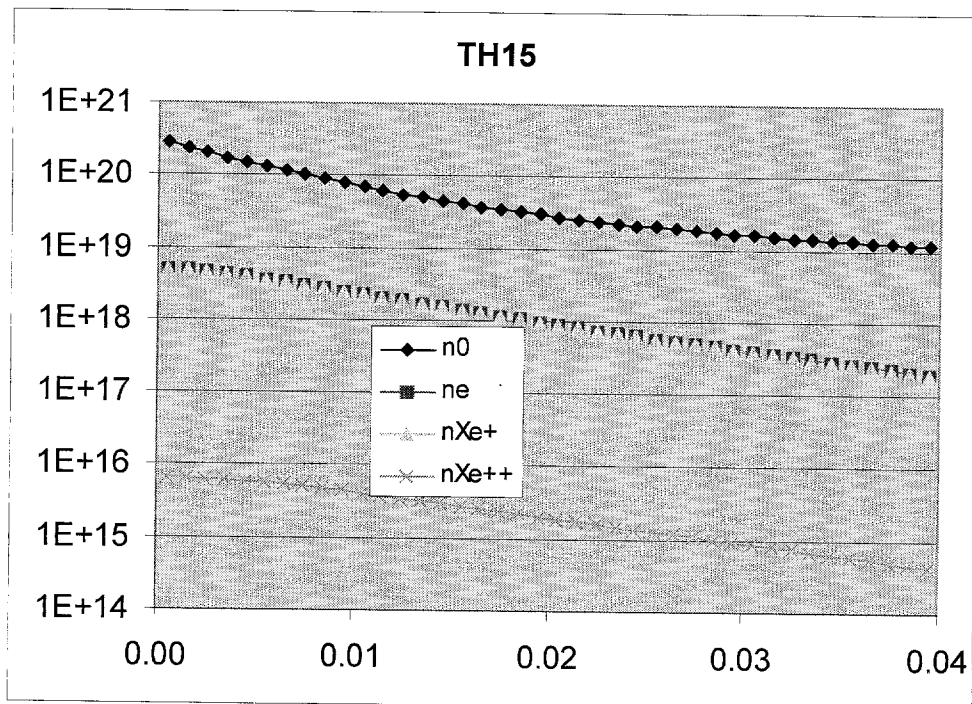


Figure 4 Model plasma densities for operating condition TH15.

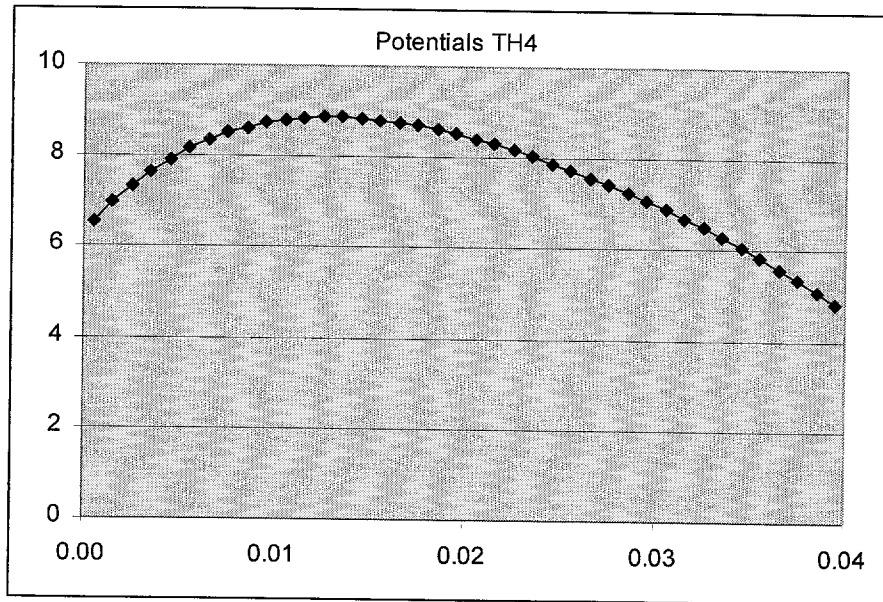


Figure 5. Model predictions of the axial potential for operating conditions TH4.

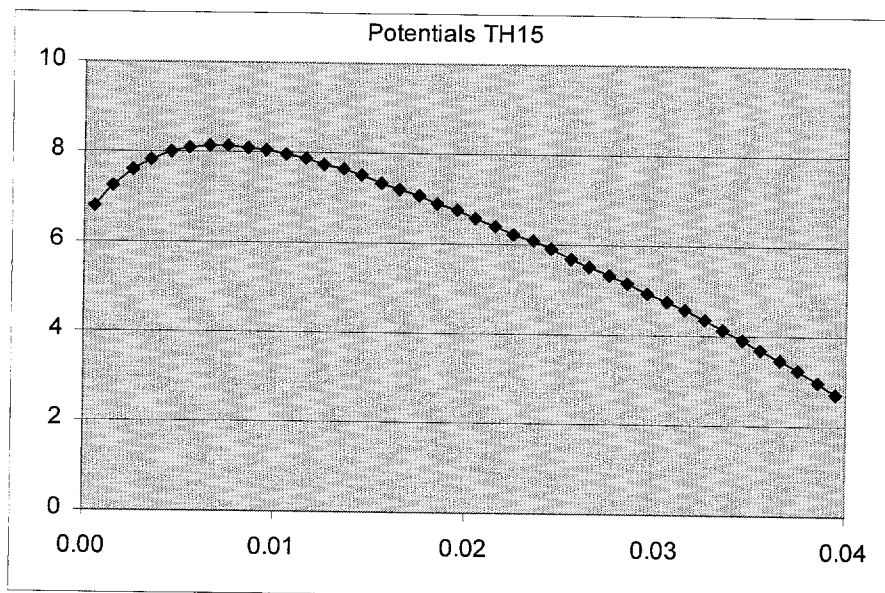


Figure 6. Model predictions of the axial potential for operating conditions TH15.

Double ion production

One surprising result of these early 1-D numerical simulations is the very low double ion production near the cathode, even at the high-power TH15 conditions. The double ion fraction is not consistent with measurements of the double ion fraction in the thruster ion beam (~10 to 25 %). The 1-D model results suggests that most of the double ions in the

beam are produced far downstream of the discharge cathode, much closer to the screen grid. As discussed earlier, the volumetric single and double ion production rates are

$$\dot{n}^+ = n_0 n_e \alpha^+(T_e)$$

$$\dot{n}^{++} = n^+ n_e \alpha^{++}(T_e)$$

Neglecting single ion losses, the ratio of currents in a volume, V , is

$$J^+ \approx e \int \dot{n}^+ dV = e \int n_0 n_e \alpha^+(T_e) dV$$

$$J^{++} = 2e \int \dot{n}^{++} dV = 2e \int n^+ n_e \alpha^{++}(T_e) dV$$

$$\frac{J^{++}}{J^+} \approx 2 \left(\frac{n^+}{n_0} \right) \left(\frac{\alpha^{++}(T_e)}{\alpha^+(T_e)} \right)$$

where J^+ and J^{++} are the single and double ion production rates (expressed as currents), respectively, in volume V .

The ratio of ionization rate coefficients, $\frac{\alpha^{++}(T_e)}{\alpha^+(T_e)}$, as a function of electron temperature is shown in Figure 7; this ratio is at most 21%. If, instead of maxwellian electrons, primary electrons produce most of the ions, the ratio of ionization rate coefficients is different; however, it is less than 50% at the typical NSTAR thruster discharge voltage (~ 25 V). The ratio never exceeds 75% at any voltage, and is zero below the xenon second ionization potential (21.2 eV).

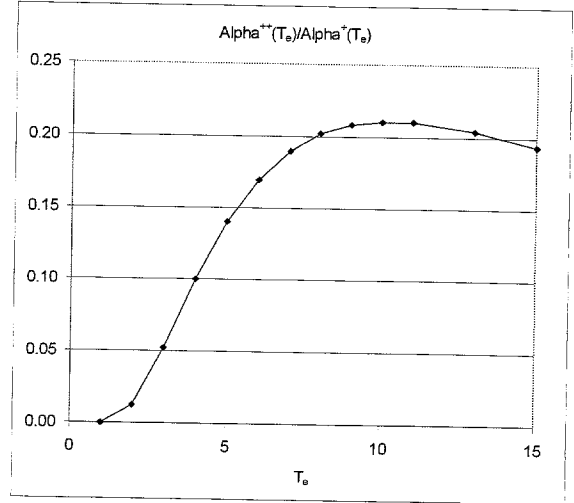


Figure 7. Ratio of single ionization to double ionization rate coefficients.

To obtain the high double ion current fraction measured in the beam extracted from the thruster, the ion density be comparable to the neutral density.

$$\left(\frac{n^+}{n_0} \right) \approx \frac{1}{2} \left(\frac{\alpha^+(T_e)}{\alpha^{++}(T_e)} \right) \frac{J^{++}}{J^+} \sim 0.6 - 0.7$$

Near the discharge cathode, the neutral density is very high, a few times 10^{20} m^{-3} , and the measured ion densities are less than 10^{19} m^{-3} . Consequently the double ion fraction is limited to a few per cent as shown in Figure 8; this is much less than the ratio measured in the beam. Near the screen grid the neutral density is much lower, and we expect that a new 2-D discharge chamber code under development¹⁶ will show that most double ions in the ion beam are generated near the screen grid. Although the double to single ion production ratio is low near the cathode keeper, the magnitude of the double ion current to the keeper may be large enough to account for the observed keeper erosion.

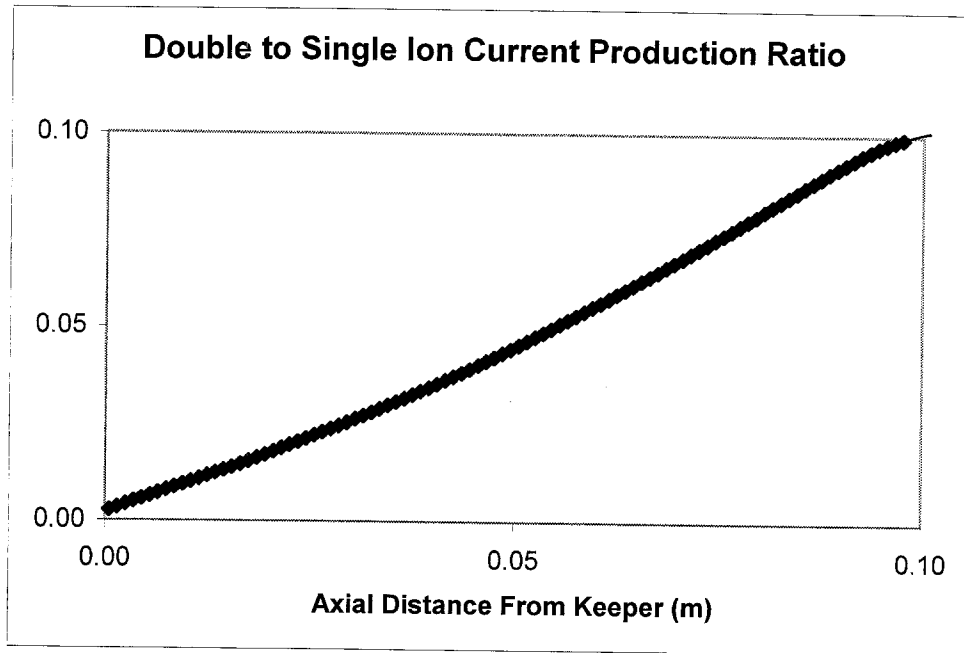


Figure 8. The ratio of double ion current to single ion current generation rates as function of distance downstream of the discharge chamber hollow cathode keeper.

Conclusions

The calculations presented here show reasonable agreement with measured ion densities reported in the literature, and the model predicts a potential hill downstream of the cathode orifice. The predicted double ion ratio near the cathode appears to be much lower than originally expected, however, these results are consistent with the low measured values in the literature in this region and are understandable based on the ionization mechanisms in the channel.

There are many concerns and limitations in using a 1-D model in this region. The electron drift velocities in the channel are generally larger than the thermal speed, a condition that can trigger electron drift instabilities. The classical scattering lengths are also a few centimeters, indicating that the fluid electron model is marginal. We plan to investigate these issues, and to develop robust and more accurate plasma

generation algorithms to use in a 2-D discharge chamber model¹⁶.

Acknowledgements

The work described in this paper was conducted by the Jet Propulsion Laboratory, California Institute of Technology, under contract to the National Aeronautics and Space Administration.

References

1. Patterson, M. J., Rawlin, V. K., Sovey, J. S., Kussmaul, M. J., Parkes, J., "2.3 kW Ion Thruster Wear Test," AIAA-1995-2516, 31st AIAA/ASME/SAE/ASEE Joint Propulsion Conference and Exhibit, San Diego, CA, July 1995.
2. Polk, J. E., Patterson, M. J., Brophy, J. R., Rawlin, V. K., Sovey, J. S., Myers, R. M., Blandino, J. J., Goodfellow, K. D., Garner, C. E., "A 1000 Hour Wear Test of the NASA NSTAR Ion Thruster," 32nd AIAA/ASME/SAE/ASEE Joint

- Propulsion Conference and Exhibit, Lake Buena Vista, FL, July 1996.
3. Polk, J. E., Anderson, J. R., Brophy, J. R., Rawlin, V. K., Patterson, M. J., Sovey, J., Hamley, J. J., "An Overview of the Results from an 8200 Hour Wear Test of the NSTAR Ion Thruster," 35th AIAA/ASME/SAE/ASEE Joint Propulsion Conference and Exhibit, Los Angeles, CA, June 1999.
 4. Polk, J. E., Kakuda, R. Y., Anderson, J. R., Brophy, J. R., Rawlin, V. K., Patterson, M. J., Sovey, J., Hamley, J., "Performance of the NSTAR Ion Propulsion System on the Deep Space One Mission," AIAA-2001-0965, 39th AIAA Aerospace Sciences Meeting and Exhibit, Reno, NV, January 2001.
 5. Sengupta, A., Anderson, J. R., Brophy, J. R., Rawlin, V. K., Sovey, J. S., "Performance Characteristics of the NSTAR Ion Thruster During an On-Going Long Duration Ground Test," IEEE 8.0303, IEEE Aerospace Conference, Big Sky, MT, March 2000.
 6. Williams, G. J., Smith, T. B., Glick, K. H., Hidaka, Y., Gallimore, A. D., "FMT-2 Discharge Cathode Erosion Rate Measurements via Laser Induced Fluorescence," AIAA-2000-3663, 36th AIAA/ASME/SAE/ASEE Joint Propulsion Conference and Exhibit, Huntsville, AL, July, 2000.
 7. Foster, J. E., Patterson, M. J., "Plasma Emission Characteristics from a High Current Hollow Cathode in an Ion Thruster Discharge Chamber," AIAA-2002-4102, 38th AIAA/ASME/SAE/ASEE Joint Propulsion Conference and Exhibit, Indianapolis, IN, July, 2002.
 8. Domonkos, M. T., Foster, J. E., Patterson, M. J., "Investigation of Keeper Erosion in the NSTAR Ion Thruster," IEPC-2001-0308, 27th International Electric Propulsion Conference, Pasadena, CA, October 2001.
 9. Kolasinski, R. D., and Polk, J. E., "Characterization Of Cathode Keeper Wear By Surface Layer Activation," AIAA-2003-5144, 39th AIAA/ASME/SAE/ASEE Joint Propulsion Conference and Exhibit, Huntsville, AL, July 20-23, 2003.
 10. Herman, D. A., McFarlane, D. S., Gallimore, A. D., "Discharge Plasma Parameters of a 30-cm Ion Thruster Measured without Beam Extraction using a High-Speed Probe Positioning System," IEPC-2003-0069, 28th International Electric Propulsion Conference, Toulouse, France, March 2003.
 11. Friedly, V. J., Wilbur, P. J., "High Current Hollow Cathode Phenomena," Journal of Propulsion and Power Vol. 8, No. 3, May-June 1992, pp. 635-643.
 12. Williams, J. D., "Plasma Contactor Research - 1990," NASA CR-187097, January 1990.
 13. Kameyama, I., Wilbur, P. J., "Measurements of Ions from High Current Hollow Cathodes Using Electrostatic Energy Analyzer," Journal of Propulsion and Power Vol. 16, No. 3, May-June 2000, pp. 529-535.
 14. Miller, J. S., Pullins, S. H., Levandier, D. J., Yu-hui, C., Dressler, R. A., "Xenon charge exchange cross sections for electrostatic thruster models," Journal of Applied Physics, Vol. 9, No. 3, 1 February 2002, pp. 984-991.
 15. Katz, I., Anderson, J. R., Polk, J. E., Brophy, J. R., "A Model of Hollow Cathode Chemistry," AIAA-2002-4241, 38th AIAA/ASME/SAE/ASEE Joint Propulsion Conference and Exhibit, Indianapolis, IN, July, 2002.
 16. Wirz, R., and Katz, I., "A 2- D Computational Model of an Ion Thruster Discharge Chamber," AIAA-2003-5163, 39th AIAA/ASME/SAE/ASEE Joint

Propulsion Conference and Exhibit,
Huntsville, AL, July 20-23, 2003.